

# <sup>11</sup>C-methionine PET for the diagnosis and management of recurrent pituitary adenomas

B. N. T. Tang<sup>1,6</sup>, M. Levivier<sup>2</sup>, M. Heurreux<sup>3</sup>, D. Wikler<sup>1</sup>, N. Massager<sup>2</sup>, D. Devriendt<sup>4</sup>, P. David<sup>5</sup>, N. Dumarey<sup>1</sup>, B. Corvilain<sup>3</sup>, S. Goldman<sup>1</sup>

<sup>1</sup> PET-Biomedical Cyclotron Unit and Department of Nuclear Medicine, Université Libre de Bruxelles, Erasme Hospital, Brussels, Belgium

<sup>2</sup> Department of Neurosurgery, Université Libre de Bruxelles, Erasme Hospital, Brussels, Belgium

<sup>3</sup> Department of Endocrinology, Université Libre de Bruxelles, Erasme Hospital, Brussels, Belgium

<sup>4</sup> Department of Radiotherapy, Jules Bordet Institute, Bordet, Brussels, Belgium

<sup>5</sup> Department of Neuroradiology, Université Libre de Bruxelles, Erasme Hospital, Brussels, Belgium

<sup>6</sup> Service of Nuclear Medicine, Erasme Hospital, Route de Lennik 808, 1070 Brussels, Belgium

Received: 11 March 2005 / Accepted: 5 June 2005 / Published online: 15 October 2005

© Springer-Verlag 2005

**Abstract.** *Purpose:* The detection of recurrent pituitary adenoma by magnetic resonance imaging (MRI) is rendered uncertain by the tissue remodelling that follows surgery or radiotherapy. We aimed to evaluate the contribution of PET with <sup>11</sup>C-methionine (MET-PET) in the detection and management of recurrent pituitary adenoma. *Methods:* Thirty-three patients with pituitary adenoma were evaluated postoperatively by MET-PET, either because of biological evidence of active residual tumour or because of MRI demonstration of non-functional adenoma growth. We studied 24 secreting adenomas and nine non-functional adenomas.

*Results:* In 30 patients, MET-PET detected abnormally hypermetabolic tissue. In 14 out of these, MRI did not differentiate between residual tumour and scar formation. In nine of these 14 cases, major therapeutic decisions were undertaken (radiosurgery and surgery). In another group of 16 patients, both MET-PET and MRI detected abnormal tissue. In one case, neither MRI nor MET-PET detected adenomatous tissue. Finally, abnormal tissue was detected in two patients on MRI solely. In these two cases, failure of MET-PET to reveal the adenoma was attributable to concomitant inhibitory therapy. The sensitivity of MET-PET and MRI varied as a function of the tumour type: all non-functional adenomas were localised by both modalities, while MET-PET detected all adrenocorticotrophic hormone-secreting adenomas whereas MRI depicted only one of these eight lesions. Fifteen out of 17 patients treated by radiosurgery showed clinical improvement after treatment. *Conclusion:* We suggest that MET-PET is a sensitive tech-

nique complementary to MRI for the detection of residual or recurrent pituitary adenomas. It should gain a place in the efficient management of these tumours.

**Keywords:** Pituitary – Adenomas – PET – Methionine – Radiosurgery

**Eur J Nucl Med Mol Imaging (2006) 33:169–178**

DOI 10.1007/s00259-005-1882-0

## Introduction

Pituitary adenomas (PAs) are relatively common tumours accounting for approximately 10–20% of all primary intracranial tumours [1, 2]. Up to 75% of all PAs present unregulated secretion of hormones that leads to three major endocrine disorders, namely hyperprolactinaemia, acromegaly and Cushing syndrome. Non-secreting (non-functional) PAs most commonly become clinically patent through their intrasellar or extrasellar extension, causing various degrees of hypopituitarism and symptomatic compression of cerebral structures such as the optic chiasma.

The primary treatment of growth hormone (GH)-secreting PAs remains surgical trans-sphenoidal adenectomy, with long-term remission rates ranging from 40% to 60% [3, 4]. Similarly, the results of resection surgery for prolactin (PRL)-secreting PAs are still highly variable, with a recurrence rate ranging from 17% to 50% [5]. Cushing syndrome caused by the inappropriate secretion of adrenocorticotrophic hormone (ACTH) is often the consequence of a secreting microadenoma [6, 7]. However, even if localisation of ACTH-secreting PAs is challenging, 70–90% remission rates have been reported [6–8]. Curative surgery of central hyperthyroidism, a rare form of hyperthyroidism related to thyroid stimulating hormone (TSH)-secreting

B. N. T. Tang (✉)  
Service of Nuclear Medicine,  
Erasme Hospital,  
Route de Lennik 808,  
1070 Brussels, Belgium  
e-mail: Thanh.Tang@ulb.ac.be  
Tel.: +32-2-5553111, Fax: +32-3-5556800

PAs, again shows wide variations among the published series [9, 10]. No reliable medical therapy for non-functional adenomas has been established. Small tumours need yearly follow-up by magnetic resonance imaging (MRI), endocrine and ophthalmological assessment. When surgical treatment becomes compulsory, its success is evaluated by clinical and imaging assessment in the postoperative period but long-term follow-up remains necessary. Tumour residues may be treated by surgery or adapted radiotherapy if their growth represents a medical threat.

Radiosurgery, in particular with the Leksell gamma-knife system (Elekta A.B., Stockholm, Sweden) (GKRS), has gained an important place in the management of brain tumours. It allows the safe destruction of a brain lesion by focussing numerous radiation beams on the abnormal brain area, while preserving the normal surrounding structures. It has been proven to be effective in the treatment of a large range of malignant and benign conditions, including PA [11, 12].

Considering the high recurrence rate after surgical treatment, the accurate evaluation of residual or recurrent secreting PAs by imaging techniques is essential. MRI, commonly used in the postoperative follow-up of PAs, presents certain limitations and is often unable to distinguish between residual tumours, postoperative remodelling [13–15] and surgical packing material [16, 17]. Since PAs are characterised by a high amino acid metabolism and consequently high uptake of  $^{11}\text{C}$ -methionine (MET), PET using MET as a tracer (MET-PET) may be a suitable method for the accurate detection of these tumours [18, 19].

Our purpose in this study was to evaluate whether high-resolution MET-PET improves the detection and management of recurrent or residual PAs, and whether this metabolic information is a convenient method for guiding GKRS treatment of these tumours. Accordingly, we evaluated PET and MRI for the detection of adenomatous lesions as well as the clinical impact of each imaging technique.

**Table 1.** Characteristics of patients with secreting PAs

Secretion	Patient no.	Serum hormone level <sup>a</sup>		Treatment at the time of MET-PET	MET	MRI	Therapeutic decision
		PRL					
PRL	1	3.0		Cabergoline 1 mg/week	L	(–)	Cabergoline
	2	34.3		–	L	(–) <sup>b</sup>	GKRS
	3	14.4		–	L	(–) <sup>b</sup>	GKRS
	4	9.0		–	R	R <sup>b</sup>	GKRS
	5	7.5		Cabergoline 1 mg/week	R	(–)	GKRS
	6	1.8		Cabergoline 0.5 mg/week	(–)	R	GKRS
	7	3.4		–	L	L	GKRS proposed
	8	5.9		–	L	L	GKRS proposed
	9	1.6		–	L	L	Surgery
	10	2.0		Cabergoline 2.5 mg/week	(–)	R	GKRS
PRL and GH	11	PRL	Somatomedin C	–	R	R <sup>b</sup>	GKRS
		4.5	1.3				
		24-h cortisol urinary secretion					
ACTH	12	N <sup>c</sup>		Ketoconazole 800 mg/day	R	(–) <sup>b</sup>	GKRS
	13	2.8		–	R	(–)	Surgery
	14	5.0		–	R	(–)	GKRS
	15	2.2		Ketoconazole 600 mg/day	R <sup>b</sup>	(–)	GKRS
	16	c		–	L	L	GKRS
	17	1.5		–	L	(–)	GKRS
	18	4.2		–	L	(–)	GKRS
	19	N <sup>d</sup>		–	L	(–)	Observation
GH	20	Somatomedin C		–	R	(–)	Somatostatin
		1.2					
		1.8					
		N <sup>d</sup>					
	22	N <sup>d</sup>		–	(–)	(–)	Cabergoline
	23	1.3		–	L <sup>b</sup>	(–)	Somatostatin
TSH	24	Elevated serum FT <sub>3</sub> , FT <sub>4</sub> ; TSH N		–	R and M	(–)	Somatostatin

N hormone level in normal ranges, (–) no pituitary adenoma identified, MET methionine, MRI magnetic resonance imaging, PRL prolactin, GH growth hormone, ACTH adrenocorticotrophic hormone, TSH thyroid-stimulating hormone, GKRS gamma-knife radiosurgery, FT<sub>3</sub> free triiodothyronine, FT<sub>4</sub> free thyroxine, L left part of pituitary region, R right part of pituitary region, M median part of pituitary region

<sup>a</sup>Hormone level expressed as the absolute level divided by the upper limit of the normal range

<sup>b</sup>Results of the reading were doubtful but were “forced” within the binary scale

<sup>c</sup>Elevated ACTH

<sup>d</sup>Dynamic test revealed persistent autonomous secretion

## Materials and methods

### Patient characteristics

This longitudinal study involved 33 patients with a clinical history of surgical ablation of pituitary adenoma performed at least 3 months before inclusion. They were 16 males and 17 females (mean age $\pm$ SD 50 $\pm$ 14 years). The patients were evaluated by MET-PET and MRI either after biological evidence of active residual/recurrent tumour or after MRI demonstration of non-functional PA growth.

Between May 2000 and October 2003, we studied 24 secreting and nine non-functional PAs. The secreting adenomas were found to produce PRL ( $n=10$ ), both PRL and GH ( $n=1$ ), ACTH ( $n=8$ ; patient no. 16 suffered from Nelson syndrome), GH ( $n=4$ ) or TSH ( $n=1$ ).

Time between trans-sphenoidal surgery (or combined trans-sphenoidal surgery and radiotherapy,  $n=2$ ) and PET acquisition was (mean $\pm$ SD) 4.3 $\pm$ 4.7 years (range 4 months to 20 years). The time interval between PET and MRI assessments was 0.23 $\pm$ 2.33 months. The stereotactic acquisition for GKRS, as described below, was performed in 10 out of 18 patients at the initial PET assessment, while the remaining eight subjects had this acquisition at a later time point after the initial diagnostic PET.

Four patients with PRL and two patients with ACTH-secreting PAs were treated with, respectively, cabergoline and ketoconazole at the time of MET-PET acquisition.

Patients' characteristics and their plasma hormone level are summarised in Tables 1 and 2.

### PET acquisition and imaging analysis

Patients in the fasted state were injected intravenously with a bolus of 555 MBq of MET prepared following a method adapted from Comar et al. [20]. The 20-min emission scans, previously described [21] as usual for brain imaging, were obtained starting 20 min post injection.

Attenuation correction was performed by means of a transmission scan. All MET-PET studies were performed on an ECAT 962-HR+ operated in 3D mode (CTI-Siemens, Knoxville, TN). This system provides a set of 63 planes with a slice thickness of 2.4 mm and an in-plane resolution (full-width at half-maximum) of 4.6 mm. The PET image analysis was done visually by the nuclear physician, with access to all biological, clinical and radiological information available. Areas of MET uptake that were located outside the likely limits

**Table 2.** Characteristics of patients with non-secreting PAs

Patient no.	Treatment at the time of MET-PET	MRI	Therapeutic decision
25	–	L	GKRS
26	–	R	Observation
27	–	M	Observation
28	–	M	GKRS
29	–	M	GKRS
30	–	R and M	Observation
31	–	L and R	GKRS proposed
32	–	R	GKRS
33	–	L	GKRS proposed

MET methionine, MRI magnetic resonance imaging, L left part of pituitary region, R right part of pituitary region, M median part of pituitary region, GKRS gamma-knife radiosurgery

of the normal gland were considered abnormal, as were zones with a relatively increased volume compared with the expected anatomical centrossellar distribution of the pituitary gland. In the 10/18 patients who had the initial PET assessment at the time of planning of a GKRS procedure, the image analysis was done in co-registration with the MRI data.

We used a binary system to interpret the PET data since they were used to provide a direct verdict on whether or not a treatment should be launched.

### MRI acquisition and imaging analysis

MRI examinations were performed using a 1.5-T whole-body MR imager (Gyrosan ACS-Power Trak 6000, Philips, Best, The Netherlands), with a maximum gradient strength of  $\pm 20$  mT/m. A standard circularly polarised head coil was used. The following sequences were acquired in each patient: sagittal and coronal and axial T1-weighted spin-echo images with imaging parameters of 450/11 (TR/TE), slice thickness of 3 mm, field of view of 150 $\times$ 200 and matrix of 205 $\times$ 256; coronal T2-weighted spin-echo images with imaging parameters of 4,500/100 (TR/TE), slice thickness of 2.5 mm, field of view of 140 $\times$ 200 and matrix of 320 $\times$ 512. We finally obtained contrast-enhanced T1-weighted gradient echo images with 20/4.6/25 $^\circ$  (TR/TE/angle), field of view 220 $\times$ 270, 100 slices and a spatial resolution of 1 mm in the three directions after intravenous injection of 0.05 mmol of gadopentetate dimeglumine per kilogram of body weight (Dotarem, Guerbet Laboratories, Aulnay-sous-Bois, France). The major criterion used for PA detection on MRI was the lower contrast enhancement after injection of gadolinium [22]. All biological and clinical information was avail-

**Table 3.** MRI findings

Patient no.	T1	T2	Contrast enhancement	Contrast enhancement in comparison with the normal pituitary gland
4	Isodense	Hypodense	+	<
6	Hyperdense	Hypodense	+	<
7	Hypodense	Hyperdense	+	<
8	Hypodense	Hypodense	+	<
9	Hypodense	Heterogeneous	+	<
10	Hypodense	Heterogeneous	+	<
11	Isodense	Isodense	+	<
16	Hypodense	Isodense	+	<
21	Hypodense	Hypodense	+	<
25	Isodense	Heterogeneous	+	<
26	Isodense	Hyperdense	+	=
27	Hypodense	Heterogeneous	+	=
28	Hypodense	Hyperdense	+	<
29	Hypodense	Hypodense	+	<
30	Hypodense	Isodense	+	<
31	Isodense	Hyperdense	+	>
32	Hypodense	Hypodense	+	<
33	Isodense	Isodense	+	=

< and >, respectively lower and higher contrast enhancement of PA in comparison with the normal pituitary gland contrast enhancement; =, contrast enhancement of PA equal to the normal pituitary gland contrast enhancement

able to the radiologist. Imaging abnormalities secondary to tumour extension, such as anatomical deviation of the pituitary infundibulum [23] and sellar floor excavation [24], were considered secondary criteria for the presence of PA. MET-PET data were not used for MRI data interpretation. As for the PET data, we used a binary system to interpret the MRI data in order to reach the therapeutic decision. The MRI findings are presented in Table 3.

#### PET integration in stereotactic GKRS procedures

The procedure of PET integration in GKRS planning has been described previously [25]. PET acquisition with the Leksell G frame attached to the patient's head has been validated using a 3D acrylic phantom containing spherical simulated targets and provides submillimetre spatial accuracy. During the PET acquisition, the stereotactic

**Table 4.** Evolution in patients treated with GKRS

Patient no.	50% isodose	Irradiated volume (mm <sup>3</sup> )	Classification	Type of PA	Follow-up (months)	Hormone levels before GKRS <sup>a</sup>	Medical treatment before GKRS	Hormone levels after GKRS	Medical treatment after GKRS
2	25	1,200	G1a	PRL	12	PRL 34.3	None	PRL 11.5	None
3	20	3,000	G1a	PRL	15.0	14.4	None	5.0	None
5	35	485	G1b	PRL	35	7.5	Cabergoline 1 mg/week	1.9	None
4	35	329	G2a	PRL	3	9.0	None	4.5	None
6	35	163	G3	PRL	No follow-up	1.8	Cabergoline 0.5 mg/week	No follow-up	No follow-up
10	35	2,600	G3	PRL	35.7	2.0	Cabergoline 2.5 mg/week	3.3	None
14	35	231	G1a	ACTH	14.5	5.0	None	7.0	None
17	35	357	G1a	ACTH	13.5	1.5	None	N	None
15	20	750	G1b	ACTH	29.5	2.2	Ketoconazole 600 mg/day	N	Ketoconazole 400 mg/day
18	35	597	G1b	ACTH	12.8	4.2	None	4.3	None
12	30	168	G1b	ACTH	11	N <sup>b</sup>	Ketoconazole 800 mg/day	N	Ketoconazole 200 mg/day
16	30	575	G2b	ACTH	13.9	b	None	c	None
22	24	5,000	G2b	GH	11	1.8	Somatomedin C	N	None
11	18	7,000	G2b	PRL and GH	12.0	4.5 1.3	PRL Somatomedin C	PRL Somatomedin C	1.3
32	20	2,100	G2a	Non-functional	12.6	–	–	Volume decreased	–
25	20	2,700	G2b	Non-functional	28.9	–	–	Volume decreased	–
28	14	9,300	G4	Non-functional	17.0	–	–	Volume unchanged	–
29	20	7,900	G2b	Non-functional	19.8	–	–	Volume unchanged	–

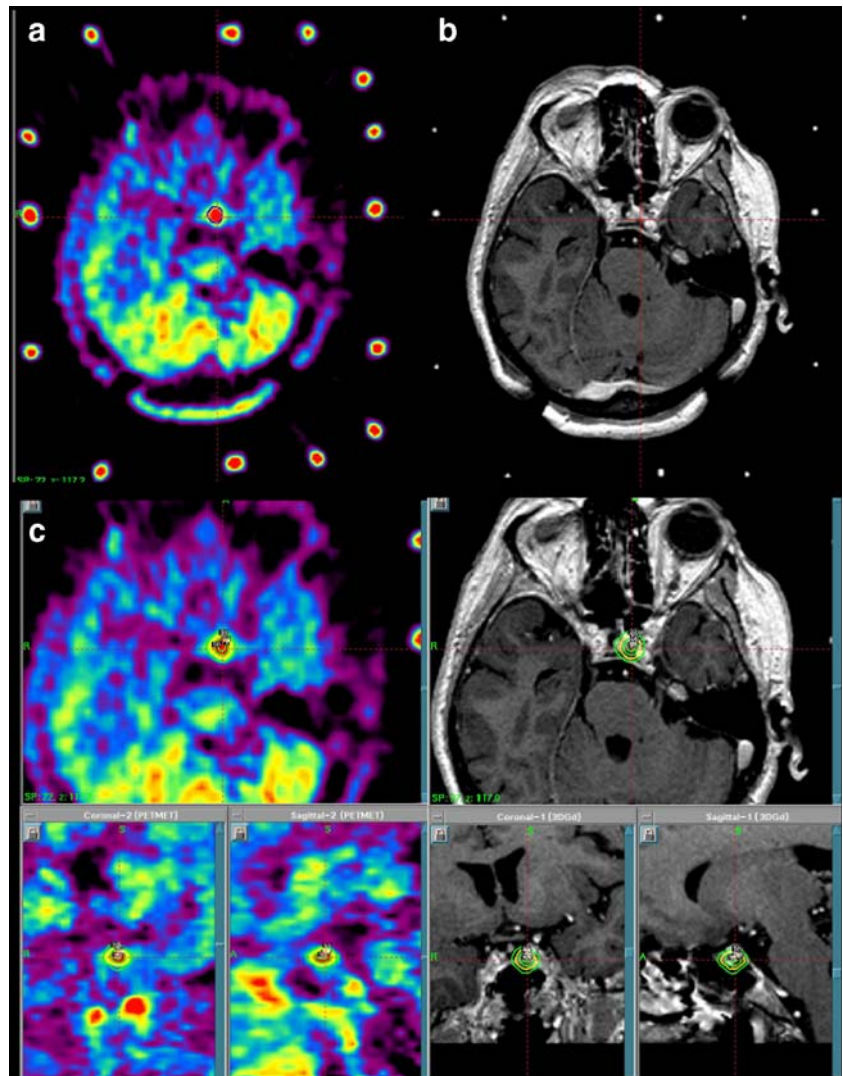
N hormone level in normal range, PA pituitary adenoma, PRL prolactin, GH growth hormone, ACTH adrenocorticotropic hormone, TSH thyroid-stimulating hormone, GKRS gamma-knife radiosurgery, FT<sub>3</sub> free triiodothyronine, FT<sub>4</sub> free thyroxine, L left part of pituitary region, R right part of pituitary region, M median part of pituitary region, (–) no pituitary adenoma identified, G1a GKRS target volume only defined on PET due to the absence of tumour signal on MRI; G1b MRI target initially not detectable, but apparent on PET-MRI co-registration, G2a target volume on PET perfectly matched MRI target volume, G2b target volumes partially matched, G3/G4 target volume only defined on MRI due to absence of tumour hypermetabolism on PET (G3) or technical problems with the PET data (G4)

<sup>a</sup>Hormone level expressed as the absolute level divided by the upper limit of the normal range

<sup>b</sup>ACTH > normal values

<sup>c</sup>ACTH in normal range

**Fig. 1.** GKRS targeting in a patient with recurrent ACTH-producing PA. On MET-PET, a hypermetabolic target is defined in the left part of the sella turcica (a). Tumour volume cannot be clearly defined on MRI (b). Prescription isodoses presented as concentric lines on transverse, sagittal and coronal MET-PET and MRI slices. The final target volume is based on the PET-defined volume transferred onto MR co-registered images (c)



frame is secured in a customised head holder originally designed for the CT scan bed. This allows fast and comparable positioning during CT, MRI and PET. Planning begins with a separate visual analysis of each stereotactic imaging modality. A 3D volumetric contour is drawn on PET images and is projected onto the corresponding MR images. The final target is drawn on the stereotactic MR images, taking into account the respective contributions of PET and MRI, as well as the anatomical location of the tumour and the functional areas at risk. In the present series, 50% isodose and volume treated were, respectively,  $27.00 \pm 7.56$  Gy and  $2,470 \pm 2,909$  mm<sup>3</sup>.

#### Statistical analysis

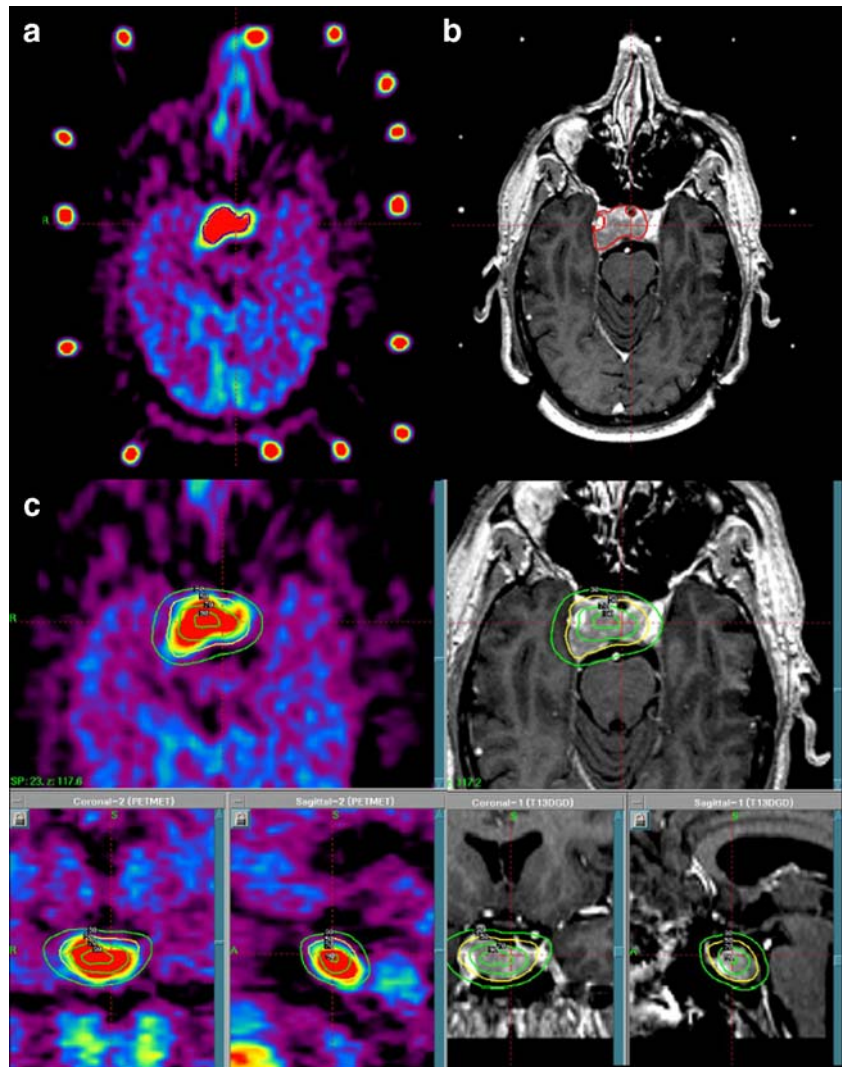
Statistical analyses were performed using Prism 2 (GraphPad Software, San Diego, CA). Spearman rank correlation test was used to analyse the relationship between MET uptake and hormone levels. The level of significance was set at  $p < 0.05$ .

## Results

### *MET-PET for the detection of residual PA*

No imaging evaluation (MRI or MET-PET) was considered “non-diagnostic”. In five MRI and two MET-PET studies (from 33 patients), the results of the reading were doubtful but forced within the binary scale (Table 1). The MET-PET assessment technique detected abnormal hypermetabolic tissue in the sellar or parasellar region in 30 cases. MRI detected recurrent PAs in 18 patients. In 14 patients in whom MET-PET showed the presence of active tumour, MRI was unable to differentiate between residual PA and scar formation. In nine of these 14 patients, major therapeutic decisions were undertaken on the sole basis of MET-PET results, namely GKRS ( $n=8$ ) and surgery ( $n=1$ ). In three patients successfully treated with a somatostatin ana-

**Fig. 2.** GKRS targeting in a patient with recurrent non-secreting PA in the sellar and parasellar region. On MET-PET a large hypermetabolic target is defined (a). A target is defined around the adenomatous tissue depicted on the MRI (b). Prescription isodoses presented as concentric lines on transverse, sagittal and coronal MET-PET and MRI slices. The final target is based on the combined volumes defined on the PET and MR co-registered images (c).



logue, MET-PET was the only imaging technique able to evaluate the drug efficacy. Additionally, 16 other patients were positive on both MET-PET and MRI and two were positive on MRI only. These two negative MET-PET results were obtained under uninterrupted dopamine agonist

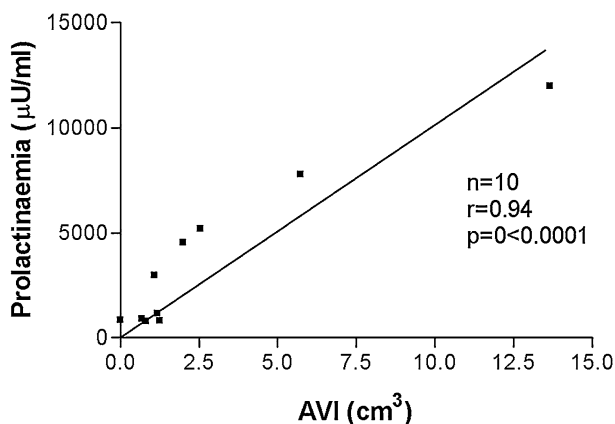


**Fig. 3.** Relation between AVI and the serum prolactin level

therapy (cabergoline) in patients who suffered from prolactinoma. When both MET-PET and MRI detected the presence of abnormal PA tissue, concordant lateralisation of tumour tissue detection was found (right, left or median part of the sella turcica).

Finally, in one case, neither MRI nor MET-PET detected adenomatous tissue. In this case, basal blood hormone levels were normal and only dynamic tests revealed a dys-regulated pituitary secretion.

#### *Combination of MET-PET with MRI for GKRS targeting*

Among the initial 33 patients included in the trial, a total of 18 were treated by a GKRS procedure planned on the basis of MET-PET and MRI stereotactic integration (Table 4). Five categories of situation were encountered following the classification previously proposed [26] and simplified for the present application: (i) target volume only defined on PET due to the absence of tumour signal on MRI (G1a) (Fig. 1); (ii) MRI target initially not detectable, but apparent on PET-MRI co-registration (G1b); (iii) target vol-

ume on PET perfectly matched MRI target volume (G2a); (iv) target volumes partially matched and consequently adjustments were made to define final therapy target (G2b) (Fig. 2); and (v) target volume was only defined on MRI owing to absence of tumour hypermetabolism on PET (G3) or technical problems with the PET data (G4). Accordingly, patients were categorised as follows: G1a subgroup,  $n=4$ ; G1b,  $n=4$ ; G2a,  $n=2$ ; G2b,  $n=5$ ; and finally G3,  $n=2$ . The conversion of PET data file format to file format used in the GKRS workstation was unsuccessful in one patient (G4).

#### *Impact of MET-PET assessment on therapeutic intervention and outcome*

Twenty-five patients were treated with GKRS ( $n=18$ ), resection surgery ( $n=2$ ) or medical therapy ( $n=5$ ). Four other patients had positive MET-PET allowing for GKRS targeting but had not yet been treated. Three patients presenting non-secreting PAs showed no sign of deterioration of the pituitary function and no sign on MRI of local invasion that could lead to compression of the optic chiasm. Consequently, a “wait and see” attitude was adopted for these patients despite the demonstration of adenomatous activity. In another patient suffering from an ACTH adenoma, incomplete suppression of cortisol secretion by 1 mg dexamethasone suggested the possibility of residual tumour; however, the 24-h cortisol urinary secretion remained within the normal range, leading to the decision to pursue careful follow-up (Table 1, patient no, 19).

Assessment of a positive response to the three treatment modalities was based on three criteria: (i) normalisation of and/or decrease in the blood hormone level, (ii) lower doses of medical treatment needed to control the disease or, finally, (iii) for the non-functional PAs, a decrease in or stabilisation of the tumour volume.

#### *Outcome in patients treated with GKRS*

Results are summarised in Table 4. Biological follow-up was available in 17 patients (G1=8, G2=7, G3=1, G4=1). The duration of the follow-up was  $17.5 \pm 9.2$  months. Six GKRS-treated patients belonging to the G1 classification had a favourable outcome. For all the GKRS-treated patients in the G2 subgroup, follow-up showed a positive response according to the criteria mentioned above. The patients belonging to the G3 and G4 subgroups had a favourable outcome. The overall success rate of GKRS was 15/17 (88%). In one patient, biological follow-up was not available but this patient, treated for PRL-secreting PA, became pregnant after GKRS (clinically favourable outcome).

Among the GKRS-treated patients, secondary effects of the treatment were limited. We observed the development of TSH insufficiency in one patient and dual TSH–ACTH insufficiency in another patient. Visual impairment after GKRS was not observed.

#### *Outcome in patients treated surgically*

Despite histological examination of the resected lesions that confirmed positive PET results, only one of the two patients was cured after surgery.

#### *Patients under medical therapy*

In three patients with secreting PAs successfully treated with a somatostatin agonist, MET-PET was the only imaging technique able to accurately evaluate the therapeutic outcome. One PRL patient, resistant to cabergoline therapy, presented persistent high uptake of MET. Finally, the patient with a GH-secreting PA that was negative on both MET-PET and MRI received inhibitory therapy.

#### *Correlation between MET uptake and hormone levels*

For the MET-PET semi-quantification, we used a thresholding technique derived from a method previously employed for the quantification of tumour load in low-grade oligodendroglioma [27]. A tumour volume was obtained in a spherical volume of interest placed around the sella turcica by automatically selecting all voxels with count values above a threshold level set at 120% of the mean cerebellar activity. To assess the tumour volume as well as its metabolic activity, an activity volume index (AVI) was calculated as the tumour volume  $\times$  (tumour mean count/cerebellum count). Using linear regression, we found a strong correlation between the AVI and the serum prolactin level ( $n=10$ ,  $r=0.94$ ,  $p<0.0001$ ) (Fig. 3). No correlation was found between the AVI and 24-h urinary cortisol level. For the GH-secreting PAs, a trend towards a correlation was found between AVI and serum IGF-1 level, but this could not be tested statistically owing to the limited number of patients ( $n=4$ ).

## **Discussion**

In this study, we have demonstrated the benefit of MET-PET for the detection and management of recurrent or residual pituitary adenoma, particularly when MRI is unable to distinguish adenomatous tissue from postoperative changes. As illustrated by our data, the clinical impact of positive MET-PET was important since it offered significant information for the planning of surgical re-intervention or radiosurgery. Hence, in GKRS procedures, MET-PET metabolic data provide essential information for dosimetry planning.

The first line of treatment for symptomatic PAs remains a therapeutic controversy. It primarily depends on the biological behaviour, the size of the tumour and the parasellar invasion. Yet, highly variable long-term outcome is reported. To provide adequate follow-up for patients suffering from PA, accurate imaging is required in order to detect recurrent or residual adenomas. MRI is convention-

ally recognised as a reference method for this purpose, but it shows major limitations consequent upon the postoperative changes at the site of the initial treatment. Early postoperative dynamic MRI has been reported to be very effective for the differentiation between residual tumour and postoperative alterations after trans-sphenoidal resection [28]. Still, for other authors [29], optimal assessment of residual tumour can only be made more than 4 months after surgery on pituitary macroadenomas. PET has previously been used for the assessment of PAs and parasellar tumours using several tracers, including FDG, MET,  $^{11}\text{C}$ -tyrosine,  $^{11}\text{C}$ -deprenyl,  $^{11}\text{C}$ -*N*-methylspiperone and  $^{11}\text{C}$ -raclopride. In particular, MET-PET appears a valuable complementary tool for the diagnosis of PA, since it adequately differentiates viable tumour from non-tumour lesions, such as fibrosis or cysts [19]. MET-PET has also been proposed for the evaluation of drug effects on prolactinomas [30].

In this study, PET delineated zones of increased MET uptake in the sellar region in 30 out of 33 patients initially suspected of having recurrent PA. Two out of the three PET-negative cases were PRL adenomas under dopamine agonist treatment, which reduced PRL secretion and therefore restrained the metabolic activity detected on PET examination [30]. The remaining PA case with negative MET-PET results was a residual GH microadenoma with low basal hormone secretion. In this case, demonstration of dysregulated GH secretion required a dynamic test. Accordingly, size and basal hormone secretion were limited and precluded the detection of residual adenomatous tissue. Indeed, as mentioned earlier, the level of hormonal secretion represents a factor of major importance for adenoma detection by MET-PET [31]. In the present study, a significant correlation between the active tumour volume and the hormone level was found for PRL-secreting PA.

In our study, the detection rate of MET-PET was very high for residual PAs, even in the so-called non-secreting or non-functional adenomas. Non-functional PAs represent a heterogeneous group of adenomas morphologically classified into two subgroups: (i) those that have hormone immunoreactivity and ultrastructural features of known adenohypophyseal cell types [10, 32, 33] and (ii) those composed of cells that do not resemble adenohypophyseal cell types [34]. The lack of hormone secretion by the immunologically reactive cell adenomas is as yet unexplained. Our demonstration of high MET uptake by all non-functional PAs favours the assumption of a high synthesis rate of incompletely processed or truncated pituitary hormones.

We report here that the detection rate of MET-PET in comparison to MRI is a function of the tumour type. While all non-functional adenomas were visualised by both modalities, MET-PET detected abnormal tissue in all eight ACTH-producing tumours, whereas only one was visible on MRI. The well-known small size of ACTH adenomas (4–5 mm) limits the ability of MRI to visualise these tumours, with the consequence that its reported sensitivity varies between 42% and 80% [35]. The high level of ACTH secretion by these microadenomas, leading to clinically patent Cushing syndrome [6], probably accounts for their high detectability by a sensitive functional imaging

modality such as MET-PET. In the majority of cases, clinical follow-up showed that this sensitive detection had a positive impact on patient management (Table 4, Fig. 4). Our group has previously demonstrated the importance of PET data for stereotactic guidance of brain biopsies [36–39], brain tumour radiosurgery or resection under neuro-navigation [26]. Here, we provide evidence that MET-PET contributes to the therapeutic management of PAs, characterised by peptidic production, fixed localisation and small size. Adding the anatomical precision of PET and MRI stereotactic co-registration to the high MET uptake rate improves GKRS targeting of PAs. The method aims at significantly increasing the proportion of patients who may be considered for GKRS treatment that is, by nature, imaging dependent. Despite this extension of GKRS indications to more difficult cases in terms of lesion detection, we achieved a percentage of therapeutic success similar to that previously reported by others [40].

$^{18}\text{F}$ -fluorodeoxyglucose (FDG) PET has been described to be useful in the diagnosis of pituitary microadenomas [41], but literature on this matter remains limited. The detection rate of PAs by FDG-PET, as reported by De Souza et al., is unsatisfactory, probably because FDG uptake is more directly related to tumour aggressiveness than to hormonal production and secretion. Unlike FDG, MET is incorporated by the normal gland and therefore could result in a higher rate of false positive results. However, we believe that the use of MRI co-registration with MET-PET assessments should avoid such an outcome as long as the anatomical structure of the normal pituitary gland is identified. An additional limitation to the MET-PET technique may be the variation in MET uptake during the menstrual cycle in women. High uptake of MET has been reported within the sella turcica of a patient immediately following abortion, thus suggesting sensitivity of MET uptake to the hormonal status in female patients [42]. Ideally, MET-PET should be planned at the constant time of the menstrual cycle, ideally at the beginning of the pre-ovulatory phase. Single-photon emission computed tomography (SPECT) using somatostatin or dopaminergic receptor ligands pres-

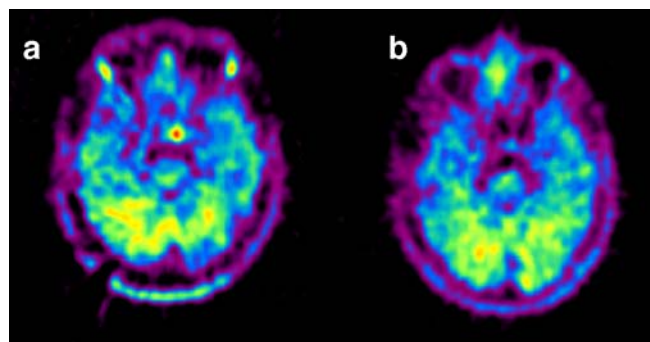


**Fig. 4.** MET-PET of an ACTH-producing PA. Before GKRS treatment, abnormal hypermetabolic tissue was present in the left part of the sella turcica, providing a target for GKRS (a). Decreased methionine uptake was observed in the target volume 13.5 months after GKRS treatment that normalised the 24-h cortisol urinary secretion (b)

ents variable accuracy for the evaluation of PAs, depending on the hormonal profile. Somatostatin is a hypothalamic inhibitor of pituitary growth hormone secretion and cell proliferation, binding to five distinct receptor subtypes (sstr1–5). In-DTPA-DPhe<sup>1</sup>-octreotide (<sup>111</sup>In-octreotide) binds tosstr2 and 5 with high affinity [43]. Human pituitary adenomas express multiple somatostatin receptor subtypes with high variability, explaining the inconsistency of <sup>111</sup>In-octreotide accuracy in detecting PAs [44, 45]. Some GH-secreting PAs and non-secreting PAs contain dopamine receptors, but the affinity and number of binding sites are significantly lower than those in PRL-secreting and non-secreting PAs [46]. SPECT using somatostatin- and dopamine-related tracers displays a high positive predictive value and consequently is informative for appropriate selection of candidates for somatostatin agonist or dopamine inhibitor treatment. The main drawback of the SPECT method remains its limited spatial resolution, insufficient for targeting a GKRS treatment. Somatostatin and dopamine receptor PET ligands have been developed, such as <sup>68</sup>Ga-DOTA-DPhe<sup>1</sup>-Tyr<sup>3</sup>-octreotide or <sup>11</sup>C-raclopride. These tracers may be developed as an appropriate tool for the targeting of GKRS treatment for PAs presenting a high density of somatostatin or dopamine receptors. Still, we consider that the use of protein synthesis markers is more suitable for the management of PAs since these tracers may be applied in all types of PA, independent of their receptor status.

Histological confirmation of MET-PET data was available in only two cases. Nevertheless, there are strong indirect arguments for considering MET-PET as an accurate tool for the detection of recurrent PA—namely, the results of therapeutic GKRS and the correlation between the disappearance of metabolically active lesions and the success of somatostatin analogue treatment. Still, it is essential to define the position of PET imaging within the armamentarium used to manage PAs. The primary diagnosis of these tumours remains essentially dependent on hormonal testing and MRI, with potential help provided by MET-PET. At recurrence, particularly when postoperative sellar changes perturb the interpretation of morphological imaging, MET-PET should gain a more preponderant role, but not independently from the other diagnostic tools. This is why in our work we have not evaluated the independent accuracy of MET-PET for the diagnosis and localisation of PAs.

## Conclusion

MET-PET usefully complements the imaging investigation of residual or recurrent PAs, whatever their secretion features. It should gain a place in the efficient management of these tumours. Because of the limitations of MRI, MET-PET provides decisive complementary information to determine the target volume in radiosurgical procedures, particularly for ACTH-secreting PAs. Finally, MET-PET provides an imaging technique for assessment of the efficacy of medical treatment for PAs.

## References

1. Kuratsu J, Takeshima H, Ushio Y. Trends in the incidence of primary intracranial tumors in Kumamoto, Japan. *Int J Clin Oncol* 2001;6:183–91
2. Ferrari G, Lovaste MG, Moresco M, Rossi G. Primary intracranial tumors. Survey of incidence in the province of Trento in the years 1977–1981. *Ital J Neurol Sci* 1985;6:191–6
3. Biermasz NR, van Dulken H, Roelfsema F. Ten-year follow-up results of transsphenoidal microsurgery in acromegaly. *J Clin Endocrinol Metab* 2000;85:4596–602
4. Swearingen B, Barker FG II, Katznelson L, Biller BM, Grinspoon S, Klibanski A, et al. Long-term mortality after transsphenoidal surgery and adjunctive therapy for acromegaly. *J Clin Endocrinol Metab* 1998;83:3419–26
5. Losa M, Mortini P, Barzaghi R, Gioia L, Giovanelli M. Surgical treatment of prolactin-secreting pituitary adenomas: early results and long-term outcome. *J Clin Endocrinol Metab* 2002; 87:3180–6
6. Mampalam TJ, Tyrrell JB, Wilson CB. Transsphenoidal microsurgery for Cushing disease. A report of 216 cases. *Ann Intern Med* 1988;109:487–93
7. Davis PC, Hoffman JC Jr, Tindall GT, Braun IF. CT-surgical correlation in pituitary adenomas: evaluation in 113 patients. *Am J Neuroradiol* 1985;6:711–6
8. Nakane T, Kuwayama A, Watanabe M, Takahashi T, Kato T, Ichihara K, et al. Long term results of transsphenoidal adenomectomy in patients with Cushing's disease. *Neurosurgery* 1987;21:218–22
9. Losa M, Giovanelli M, Persani L, Mortini P, Faglia G, Beck-Peccoz P. Criteria of cure and follow-up of central hyperthyroidism due to thyrotropin-secreting pituitary adenomas. *J Clin Endocrinol Metab* 1996;81:3084–90
10. Sano T, Yamada S. Histologic and immunohistochemical study of clinically non-functioning pituitary adenomas: special reference to gonadotropin-positive adenomas. *Pathol Int* 1994;44: 697–703
11. Sheehan JP, Kondziolka D, Flickinger J, Lunsford LD. Radiosurgery for residual or recurrent nonfunctioning pituitary adenoma. *J Neurosurg* 2002;97:408–14
12. Shin M. Gamma knife radiosurgery for pituitary adenoma. *Biomed Pharmacother* 2002;56 Suppl 1:178s–81s
13. Kremer P, Forsting M, Hamer J, Sartor K. MR imaging of residual tumor tissue after transsphenoidal surgery of hormone-inactive pituitary macroadenomas: a prospective study. *Acta Neurochir Suppl* 1996;65:27–30
14. Kremer P, Forsting M, Ranaei G, Wuster C, Hamer J, Sartor K, et al. Magnetic resonance imaging after transsphenoidal surgery of clinically non-functional pituitary macroadenomas and its impact on detecting residual adenoma. *Acta Neurochir (Wien)* 2002;144:433–43
15. Rodriguez O, Mateos B, de la Pedraja R, Villoria R, Hernando JI, Pastor A, et al. Postoperative follow-up of pituitary adenomas after trans-sphenoidal resection: MRI and clinical correlation. *Neuroradiology* 1996;38:747–54
16. Steiner E, Knosp E, Herold CJ, Kramer J, Stiglbauer R, Staniszewski K, et al. Pituitary adenomas: findings of postoperative MR imaging. *Radiology* 1992;185:521–7
17. Kaiser WA, Steckelbroeck V, Siewert B, Layer G, Hochstetter A, Reiser M. Differentiating between tumor and implant material in the postoperative sella using MRT. *Rofu* 1993;158: 555–64
18. Battistin L, Gerstenbrand F. PET and NMR: new perspectives in neuroimaging and in clinical neurochemistry. New York: Liss; 1986. p. 407–24

19. Bergstrom M, Muhr C, Lundberg PO, Langstrom B. PET as a tool in the clinical evaluation of pituitary adenomas. *J Nucl Med* 1991;32:610–5
20. Comar D, Cartron J, Maziere M, Marazano C. Labelling and metabolism of methionine-methyl-<sup>11</sup>C. *Eur J Nucl Med* 1976; 1:11–4
21. Goldman S, Levivier M, Pirotte B, Brucher JM, Wikler D, Damhaut P, et al. Regional methionine and glucose uptake in high-grade gliomas: a comparative study on PET-guided stereotactic biopsy. *J Nucl Med* 1997;38:1459–62
22. Sakamoto Y, Takahashi M, Korogi Y, Bussaka H, Ushio Y. Normal and abnormal pituitary glands: gadopentetate dimeglumine-enhanced MR imaging. *Radiology* 1991;178:441–5
23. Peck WW, Dillon WP, Norman D, Newton TH, Wilson CB. High-resolution MR imaging of pituitary microadenomas at 1.5 T: experience with Cushing disease. *Am J Roentgenol* 1989; 152:145–51
24. Cano A, Martinez M, Benito P, Tofe S, Higuera A, Munoz R. Analysis of indirect signs of microprolactinoma at MR imaging. *Eur J Radiol* 1999;31:157–64
25. Levivier M. Integration of metabolic data by positron emission tomography in image-guided neurosurgical interventions [in French]. *Bull Mem Acad R Med Belg* 2002;157:235–45; discussion 245–50
26. Levivier M, Massager N, Wikler D, Lorenzoni J, Ruiz S, Devriendt D, et al. Use of stereotactic PET images in dosimetry planning of radiosurgery for brain tumors: clinical experience and proposed classification. *J Nucl Med* 2004;45:1146–54
27. Tang BN, Sadeghi N, Branle F, De Witte O, Wikler D, Goldman S, et al. Semi-quantification of methionine uptake and flair signal for the evaluation of chemotherapy in low-grade oligodendroglioma. *J Neurooncol* 2005;71:161–8
28. Yoon PH, Kim DI, Jeon P, Lee SI, Lee SK, Kim SH. Pituitary adenomas: early postoperative MR imaging after transsphenoidal resection. *Am J Neuroradiol* 2001;22:1097–104
29. Rajaraman V, Schulder M. Postoperative MRI appearance after transsphenoidal pituitary tumor resection. *Surg Neurol* 1999; 52:592–8; discussion 598–9
30. Bergstrom M, Muhr C, Lundberg PO, Bergstrom K, Gee AD, Fasth KJ, et al. Rapid decrease in amino acid metabolism in prolactin-secreting pituitary adenomas after bromocriptine treatment: a PET study. *J Comput Assist Tomogr* 1987;11: 815–9
31. Muhr C, Bergstrom M. Positron emission tomography applied in the study of pituitary adenomas. *J Endocrinol Invest* 1991; 14:509–28
32. Scippo ML, Beckers A, Franken F, Reznik M, Stevenaert A, Igout A, et al. Adenohypophysis hormone gene products in 14 pituitary adenomas: analysis by immunohistochemistry and northern blotting. *Arch Int Physiol Biochim Biophys* 1991; 99:135–40
33. Jameson JL, Klibanski A, Black PM, Zervas NT, Lindell CM, Hsu DW, et al. Glycoprotein hormone genes are expressed in clinically nonfunctioning pituitary adenomas. *J Clin Invest* 1987;80:1472–8
34. Yeh PJ, Chen JW. Pituitary tumors: surgical and medical management. *Surg Oncol* 1997;6:67–92
35. Buchfelder M, Nistor R, Fahlbusch R, Huk WJ. The accuracy of CT and MR evaluation of the sella turcica for detection of adrenocorticotrophic hormone-secreting adenomas in Cushing disease. *Am J Neuroradiol* 1993;14:1183–90
36. Levivier M, Goldman S, Bidaut LM, Luxen A, Stanus E, Przedborski S, et al. Positron emission tomography-guided stereotactic brain biopsy. *Neurosurgery* 1992;31:792–7; discussion 797
37. Levivier M, Goldman S, Pirotte B, Brucher JM, Baleriaux D, Luxen A, et al. Diagnostic yield of stereotactic brain biopsy guided by positron emission tomography with [<sup>18</sup>F]fluorodeoxyglucose. *J Neurosurg* 1995;82:445–52
38. Levivier M, Wikier D, Goldman S, David P, Metens T, Massager N, et al. Integration of the metabolic data of positron emission tomography in the dosimetry planning of radiosurgery with the gamma knife: early experience with brain tumors. Technical note. *J Neurosurg* 2000;93 Suppl 3:233–8
39. Goldman S, Levivier M, Pirotte B, Brucher JM, Wikler D, Damhaut P, et al. Regional glucose metabolism and histopathology of gliomas. A study based on positron emission tomography-guided stereotactic biopsy. *Cancer* 1996;78:1098–106
40. Brada M, Ajithkumar TV, Minniti G. Radiosurgery for pituitary adenomas. *Clin Endocrinol (Oxf)* 2004;61:531–43
41. De Souza B, Brunetti A, Fulham MJ, Brooks RA, DeMichele D, Cook P, et al. Pituitary microadenomas: a PET study. *Radiology* 1990;177:39–44
42. Hanakawa K, Ikeda H, Ishii K, Asamoto S, Iwata T, Matsumoto K, et al. High uptake on <sup>11</sup>C methionine PET scan in the pituitary gland of a patient with cerebral glioma after surgical abortion [in Japanese]. *No To Shinkei* 1998;50:573–7
43. Virgolini I, Britton K, Buscombe J, Moncayo R, Paganelli G, Riva P. In- and Y-DOTA-lanreotide: results and implications of the MAURITIUS trial. *Semin Nucl Med* 2002;32:148–55
44. Colao A, Lastoria S, Lombardi G. Receptor imaging in the diagnosis and treatment of pituitary tumors. *J Endocrinol Invest* 1999;22:736–7
45. Boni G, Ferdeghini M, Bellina CR, Matteucci F, Castro Lopez E, Parenti G, et al. [<sup>111</sup>In-DTPA-D-Phe]-octreotide scintigraphy in functioning and non-functioning pituitary adenomas. *Q J Nucl Med* 1995;39:90–3
46. Koga M, Nakao H, Arao M, Sato B, Noma K, Morimoto Y, et al. Demonstration of specific dopamine receptors on human pituitary adenomas. *Acta Endocrinol (Copenh)* 1987;114:595–602